Temperature dependence of vicinal Si(111) surfaces

R. J. Phaneuf, Ellen D. Williams, and N. C. Bartelt
Department of Physics and Astronomy, University of Maryland, College Park, Maryland 20742
(Received 17 December 1987)

Using low-energy electron diffraction, we have examined the temperature dependence of the structure of surfaces of Si which are misoriented from the (111) plane. Our observations are on surfaces misoriented by 4° to 12° toward or away from the $[\bar{1}10]$ direction and by 6° toward the $[\bar{2}11]$. At high temperatures all these surfaces contain a uniform density of steps which have heights approximately equal to the distance between pairs of neighboring Si(111) planes. At low temperatures, the surfaces break up into two types of regions: one without steps but with a (7×7) reconstruction, the other with a high step density. This phase separation is reversible. We interpret our results in terms of the formation of a sharp edge in the equilibrium crystal shape. We support this picture by showing that the orientation of the stepped regions at low temperatures is independent of the net misorientation: all the data fall on the same temperature-orientation phase diagram. The sharp edge appears to vanish at the same temperature as the (7×7) to "(1×1)" transition on the unstepped (111) surface. We suggest a thermodynamic mechanism for this coincidence. On the surfaces misoriented toward or away from the $[\bar{1}10]$ direction, when the temperature is lowered approximately 200 °C below the temperature of the (7×7) to "(1×1)" transition, we find evidence for the beginning of a region of coexistence between two types of stepped surfaces; one with an ordered array of kinks, misoriented towards an azimuth slightly away from the $[\bar{1}10]$ direction, and the other with poor step order misoriented towards the $[\bar{1}2\bar{1}]$ direction.

INTRODUCTION

It is expected that not all surfaces which might bound a three-dimensional crystal are thermodynamically stable,[1] especially at low temperature. The stable surface orientations of a crystal are those orientations tangent to a plot of the equilibrium crystal shape. When not all orientations are allowed, the equilibrium crystal shape contains sharp edges and corners. Attempts to prepare surfaces in unstable orientations can lead to a separation of the surface into coexisting regions of stable orientation.[2] This type of surface is commonly referred to[1,2] as "faceted," or as a surface with a "hill and valley" structure. In this paper we report on measurements which suggest that a sharp edge on the boundary of the (111) facet of the silicon equilibrium crystal shape exists at low temperature, but vanishes reversibly as the temperature is raised though the (7×7) to "(1×1)" reconstructive transition temperature on the (111) facet; in particular we present the temperature dependence of the range of stable orientations of Si surfaces misoriented from the (111) plane towards or away from the $[\bar{1}10]$ direction.

In invoking properties of the equilibrium crystal shape to explain experimental data one must exercise much caution: Only a very few direct quantitative studies of equilibrium crystal shapes have been made.[3] The problem, of course, is usually that limitations on mass transport across the surface do not allow the attainment of thermal equilibrium. Kinetics limits the size of facets on a faceted surface, for example. If thermodynamics is to be used to describe the properties of the facets they should be large, otherwise finite-size effects will play a role.[1] Fortunately, scanning electron microscopy observations[4] suggest that this is the case for the types of facets whose temperature-dependent orientation we measure.

The case of Si(111) vicinal surfaces is particularly interesting because of the (7×7) reconstruction of the (111) surface. Scanning tunneling microscopy[5] as well as electron microscopy[6,7] results suggest that the (7×7) reconstruction extends right up to the edges of atomic steps on the surface, and that the reconstruction influences the configuration of step edges. The recent dimer-adatom-stacking fault model[8] includes an array of dimer chains, separating stacking faulted regions and unfaulted regions, which might interact with step edges of a particular orientation on a vicinal (111) surface. Finally, it seems likely that the presence of a high density of steps on a vicinal surface should alter the intrinsic surface stress which has been discussed by several authors[9–11] as being important in determining the reconstruction. All these results suggest some type of interaction between steps and the (7×7) reconstruction. The exact nature of the interaction may be expected to vary with the orientation of the step edges. Some possible orientations of step edges are illustrated in Fig. 1 for an unreconstructed (111) surface. Misorientation towards the $\langle 1\bar{1}0\rangle$ directions results in a low symmetry step edge. Misorientation toward the inequivalent $\langle\bar{2}\,1\,1\rangle$ or $\langle 2\,\bar{1}\,\bar{1}\rangle$ directions results in a close-packed step-edge geometry, which is also parallel to the edges of the (7×7) unit cell.

In previous low-energy electron diffraction (LEED) studies of Si(111) surfaces misoriented toward the $[\bar{2}11]$ and $[2\,\bar{1}\,\bar{1}]$ directions, phase transitions involving changes in the step height have been reported.[12] We have also investigated surfaces misoriented along these directions, and find that the energy dependence of the diffracted beam shapes indicates this interpretation to be

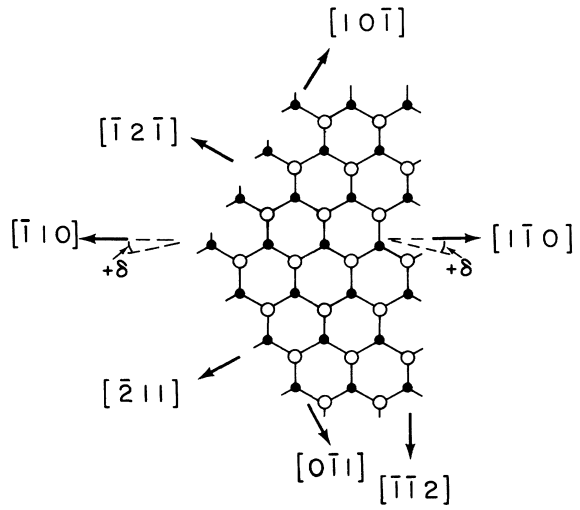

FIG. 1. Schematic drawing of the top double layer of unreconstructed Si(111) with upper Si atoms shown as open circles and lower Si atoms as closed circles. The geometry of three types of step edges is shown. Misorientation toward the $\pm[1\bar{1}0]$ directions results in a low symmetry step edge structure. Misorientation toward the $[\bar{2}11]$ or equivalent $[11\bar{2}]$ and $[1\bar{2}1]$ directions (i.e., toward a $\{110\}$ plane) results in one broken bond per edge atom. Misorientation toward the $[\bar{1}2\bar{1}]$ or equivalent $[2\,\bar{1}\,\bar{1}]$ and $[\bar{1}2\bar{1}]$ directions results in a step edge with two broken bonds per edge atom. Rotation by 30° in the $+\delta$ direction shown from the $[\bar{1}10]$ direction is required to form a $[\bar{2}11]$-type step edge.

incorrect for the $[\bar{2}11]$ direction. The behavior of surfaces misoriented toward the $\langle 11\bar{2}\rangle$ is similar to that for $\langle 1\bar{1}0\rangle$ directions of misorientation and will be discussed here. The results for surfaces misoriented toward the $\langle \bar{1}\,\bar{1}\,2\rangle$ will be presented elsewhere. Some of the results discussed here for the $[1\bar{1}0]$ misorientations have been described in two short publications.[13,14] In this paper we present a more complete account of the experiment and analysis, results for surfaces misoriented toward the $[\bar{2}11]$, and also some new results at lower temperatures which show effects of the three-dimensional nature of the equilibrium crystal shape.

The organization of the paper is as follows. First we briefly describe our experimental procedure. We then discuss our observations of the high-temperature single-phase region which is common to all the studied misorientations. Finally, we describe our detailed observations which suggest two-phase (and possibly three-phase) coexistence at lower temperatures.

EXPERIMENT

Our experiments were performed on Si single crystals that had surfaces of five different orientations. Four were oriented toward or away from an azimuth within a few degrees of the $[\bar{1}10]$ direction. (Henceforth we will use the shorthand $\pm[\bar{1}10]$ to include $[\bar{1}10]$ and $[1\bar{1}0]$.) These surfaces were misoriented by 4°, 6°, 10°, and 12° from the (111) plane. The other surface was misoriented by 6° toward the $[\bar{2}11]$ direction. The samples were mechanically polished, but not chemically etched. The doping was n type, and the resistivity was 10–50 Ω cm.

The samples were cleaned by briefly heating in ultrahigh vacuum ($p < 2\times10^{-10}$ Torr) to 1250 °C, using radiation and electron bombardment from a W-wire heater positioned behind the sample. No impurity peaks were observable in the Auger-electron spectrum following this treatment, indicating an upper limit of approximately 0.1% surface impurity concentration. Heating to temperatures below this resulted in a surface which was contaminated with carbon and also showed poorly resolved step structure-associated diffraction features. After a few seconds at 1250 °C, the electron bombardment was turned off, and heating was via radiation power alone. This was sufficient to hold the sample temperature above 900 °C. Sample temperature was monitored by a W-(5 at.%-Re)–W-(26 at.%-Re) thermocouple clamped near the edge of the sample. The thermocouple was calibrated against a pyrometer at temperatures where the Si surface was radiant. We estimate the relative uncertainty in our temperature measurements to be ±2 °C and the absolute uncertainty to be ±25 °C. While heating or cooling between taking data, the temperature was varied at approximately 0.2°C/sec. At 900 °C no temperature gradient could be observed near the sample center across distances approximately twice the electron beam diameter.

The surface structure was probed with a low-energy electron diffraction (LEED) system using a commercial four-grid optics. Measurements of diffracted beam profiles were made by imaging the diffraction pattern onto a silicon-intensified vidicon screen. The transfer width of this system is approximately 100 Å. The profiles were integrated over the intensity perpendicular to the scan direction by using an aperture width that was a few times the apparent full width at half maximum of the features being scanned.

HIGH-TEMPERATURE RESULTS

Figure 2 shows the LEED pattern we observe at 845 °C for a surface misoriented by 6° towards the $[1\bar{1}0]$ direc-

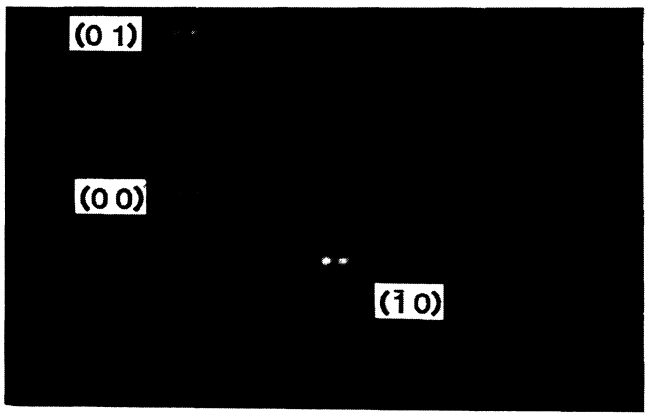

FIG. 2. LEED pattern from Si(111) misoriented by 6° toward $[1\bar{1}0]$ at 845 °C. Incident energy is equal to 47 eV; incident angle is equal to 7° from the [111] direction.

tion. It has (1×1) symmetry with splittings around the (111) surface integer-order beam positions. The splittings are dependent on the incident electron energy, as would be expected for a surface containing steps. The kinematic, or single scattering, approximation for diffraction from surface atoms arranged in a perfectly periodic monotonic staircase yields a simple form for the diffracted intensity,[15,16] which comes from the convolution theorem. The intensity can be regarded as coming from the intersection of two sets of "rods" in reciprocal space. The first set of reciprocal lattice rods is associated with the lattice of step edges. These rods are oriented perpendicular to the average surface and are spaced along the "staircase" direction at intervals of 2π divided by the separation between step edges. We refer to these as "staircase reciprocal-lattice rods." The second set comes from the basis of atoms comprising a single terrace. These "terrace reciprocal-lattice rods" are oriented normal to the terraces and are centered at the two-dimensional reciprocal-lattice points corresponding to the periodicity within a terrace. The terrace reciprocal lattice rods are broadened along the staircase direction due to the finite size of the terrace: Their first zeros are at the two-dimensional terrace reciprocal-lattice points $\pm2\pi$ divided by the terrace width. Varying the electron energy at a fixed incident direction probes the diffracted intensity along the intersecting rods, as the radius of the Ewald sphere changes. Measuring the positions of the diffracted beams in the vicinity of a terrace reciprocal-lattice rod as a function of energy thus allows the determination of the spacing between staircase reciprocal lattice rods and the angle α they make with respect to the terrace normals, and, therefore, the staircase period and step height. Two special cases are (1) in-phase conditions at which a staircase reciprocal-lattice rod intersects the center of a terrace rod, and (2) out-of-phase conditions at which two staircase rods intersect a terrace rod at positions equally displaced from its center. These conditions result in an unsplit and a symmetrically split diffracted beam, respectively. At an in-phase condition the phase difference between the scattering from successive terraces is equal to an integral number of electron wavelengths, so that the diffraction is insensitive to the presence of steps on the surface. At an out-of-phase condition the phase difference between scattering from adjacent terraces is an odd number of electron half wavelengths. Since the translation vector which connects equivalent points on adjacent terraces cannot generally be written as an integral combination of the surface unit vectors, inequivalent beams have in-phase and out-of-phase conditions at different perpendicular components of the momentum transfer.

Figure 3 shows the energy dependence of a profile through the specular beam position along the $[1\bar{1}0]$ direction at 916 °C. The observed energy dependence is characteristic of well-ordered arrays of steps. Calculated in-phase and out-of-phase conditions for steps of height equal to the Si(111) interplanar spacing of 3.135 Å are indicated in the figure. By analyzing the magnitude and energy dependence of splittings of a number of integer-order beams, we deduce an average step height of

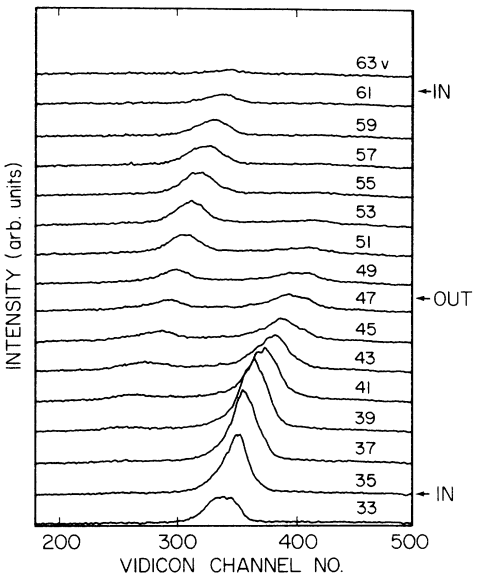

FIG. 3. Profiles of the specular beam measured along the $[1\bar{1}0]$ direction at 916 °C. Conversion of the vidicon channel number to reciprocal space position is energy dependent, scaling roughly like $E^{-1/2}$. For this figure, and Fig. 5, at 49 eV the conversion is 134 channel numbers $=|\mathbf{a}^*|/7$, where $\mathbf{a}^*$ is the first-order reciprocal-lattice vector of the (111) surface, whose magnitude is 1.89 Å^{-1}. Angle of incidence is 7°.

3.12 ± 0.07 Å, very close to the interplanar spacing, and an average step width of 28.4 ± 1.6 Å, consistent with the nominal 6° angle of cut and the observed step height.[13] A slight broadening of the peaks at the out-of-phase conditions indicates some spread in the distribution of the spacings between steps. All of the studied misorientations had similar high-temperature behavior, with the magnitude of the splitting varying as expected with the angle of cut.

Although the $[1\bar{1}0]$ and $[\bar{1}10]$ directions are mirror images, the (111) surface is threefold, not sixfold symmetric. As illustrated in Fig. 1 a 30° rotation in the positive right-hand sense about [111] from $[\bar{1}10]$ yields $[\bar{2}11]$; a similar rotation from $[1\bar{1}0]$ yields $[2\,\bar{1}\,\bar{1}]$, which is inequivalent. (Surfaces misoriented from (111) towards $[\bar{2}11]$ or $[2\,\bar{1}\,\bar{1}]$ would contain steps with one or two broken bonds per edge atom, respectively.) Distinguishing between $[\bar{1}10]$ and $[1\bar{1}0]$ is possible by observation of the energies, for a given incident direction, at which inequivalent nonspecular beams go through in-phase and out-of-phase conditions. By performing a calculation similar to that of Ref. 16, and noting the direction of satellite motion relative to the integer-order positions with energy, we find that the 4°, 10°, and 12° surfaces investigated are misoriented toward $[\bar{1}10]$, while the 6° sample is misoriented toward $[1\bar{1}0]$. Small deviations $\pm\delta$ (see Fig. 1) with respect to the direction of misorientation were observed for all the samples; for the 4° sample $\delta=-5.0°$, for the 6° sample $\delta=-0.5°$, for the 10° sample $\delta=+1.0°$, and for the 12° sample $\delta=-1.5°$.

The sample nominally misoriented toward the $[\bar{2}11]$

showed a splitting direction roughly 30° from that shown in Fig. 2. The direction of misorientation was found to deviate from the $[\bar{2}11]$ by 6°. The energy dependence was consistent with steps of height equal to one interplanar spacing, in agreement with the observations at high temperatures of previous workers.[12]

EVIDENCE FOR PHASE SEPARATION NEAR THE RECONSTRUCTION TRANSITION

Figure 4 shows the temperature dependence of the diffracted intensity around the specular beam position for a sample misoriented by 6° towards the $[1\bar{1}0]$ direction. Above a well-defined temperature ($\sim$820 °C) the magnitude of the splitting, and its dependence on energy, is temperature independent. Below this temperature a peak appears at the (111) surface specular and other integer-order beam positions and the split beams move continuously farther apart. Simultaneously, intensity appears in the seventh-order beams. The new integer- and seventh-order beams do not show the dependence on incident electron energy characteristic of diffraction from stepped surfaces; i.e., we do not resolve a periodic splitting or broadening of the angular profiles through these beams as the perpendicular component of the momentum transfer is varied. Figure 5 shows the energy dependence for angular profiles across the specular beam along the $[1\bar{1}0]$ direction at 797 °C for a 6° misoriented surface. Similar

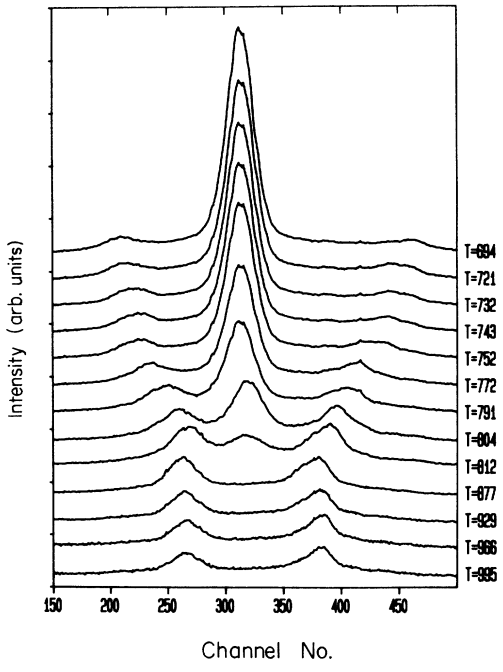

FIG. 4. Angular profiles of the specular beam in the direction of splitting as a function of temperature. Incident energy is equal to 47 eV, incident angle is equal to 8°. At this energy, 141 channel numbers are equal to $|a^*|/7$. The asymmetry of the split beams around the specular beam occurs because the incident energy is slightly less than the energy for out-of-phase scattering.

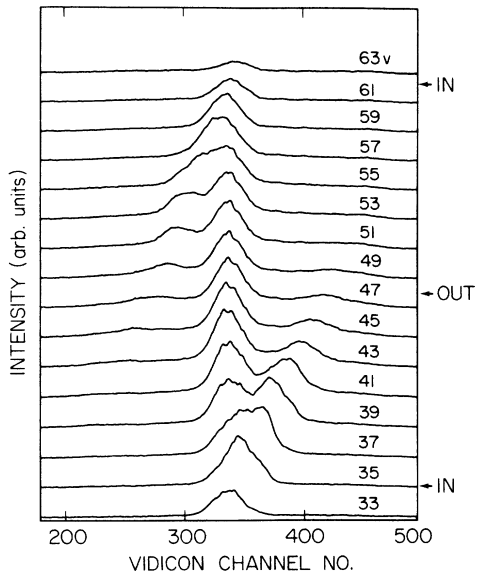

FIG. 5. Angular profiles across the specular beam for a sample misoriented by 6° toward the $[1\bar{1}0]$, at 797 °C. Same experimental conditions as Fig. 3.

measurements were also made for the (10) and $(1\bar{1})$ beams, and yielded consistent results. The peak centered at the integer-order position remained at the integer-order position as the energy was varied. The positions of the split peaks relative to the integer-order positions in all cases show the same energy dependence as above the transition (compare Figs. 3 and 5), although their separation is greater. Thus the step height has not changed although the step separation has decreased. These results suggest that the surface consists of two coexisting phases: one phase consisting of a uniform density of steps, giving rise to the split beams, the other consisting of (111) facets with (7×7) reconstruction, giving rise to the unsplit integer- and seventh-order beams. Again the split beams are broadened at out-of-phase conditions, indicating some disorder in the step position distribution.

All of the surfaces misoriented towards or away from the $[1\bar{1}0]$ directions behaved qualitatively similarly except that the temperature of the transition decreased with increasing angle of misorientation. As is illustrated in Fig. 6 for the 12° misoriented sample, the appearance of the unsplit integer-order beam and the accompanying (7×7) reconstruction occur simultaneously at $\sim$750 °C. For the 4° and 6° surfaces, the temperature dependence was completely reversible if heating and cooling rates were less than 0.2 °C/sec. Small hysteresis loops in the temperature dependence of the intensities and the beam splittings, and a slight broadening of the integer-order beams at out-of-phase conditions (observed only for the larger misorientations) will be discussed in later sections.

As Fig. 4 shows, the magnitude of the specular beam splitting along the $[1\bar{1}0]$ direction increases with decreasing temperature. This means that the average step separation on the stepped parts of the surface is decreasing; thus, since the observed average step height is approxi-

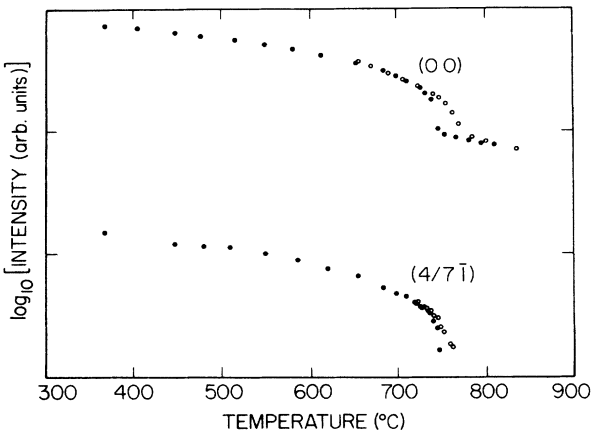

FIG. 6. Logarithm of the intensity at the specular beam position and of a seventh-order beam as a function of temperature on the surface misoriented by 12° toward [1̄10]. The specular beam intensity was measured at an out-of-phase condition. The seventh-order intensity is measured above the thermal diffuse intensity background. Closed circles measured on cooling, open circles measured on heating.

mately constant the angle of misorientation of the stepped parts of the surface is increasing. Figure 7 shows the temperature dependence of the misorientation angle α derived from the observed splittings for the 4°, 6°, and 12° net (high-temperature) misorientations. The magnitude of the splitting, and thus α, was determined by mapping the energy dependent positions of the satellite beams into reciprocal space positions using the Ewald construction. In reciprocal space the satellite positions lie along straight lines inclined by α with respect to the [111] direction. This procedure allowed for a more accurate determination of α than a single measurement at an out-of-phase condition since the satellites are more intense near an in-phase condition, and also since it averages out small errors due to inhomogeneities in the LEED optics.

Surfaces misoriented by 6° towards the [2̄11] direction behaved in qualitatively the same manner as surfaces misoriented towards or away from the [1$\bar{1}$0] direction. The temperature variation of the beam profile is qualitatively the same as in Figs. 4 and 6. The energy dependence below the transition is shown in Fig. 8. As in Fig. 5 there is an intensity component which has an energy-dependent position, and a component which does not. The energy dependence of the positions of the split beams is again consistent with a regular array of steps a single (111) interplanar spacing high. Figure 9 shows the temperature dependence of the angle of orientation of the stepped parts of the surface: It is qualitatively the same as Fig. 7. This temperature dependence was reversible if the heating and cooling rates were less than 0.2 °C/sec. Below approximately 700 °C the uncertainties in the beam splitting determination are large due to the incomplete resolution of the split beams with the nearby seventh-order beams near out-of-phase conditions and with the integer-order beams near in-phase conditions. The low-temperature limit of the orientation is roughly [113]; however, the broadened peak shapes we observe at out-

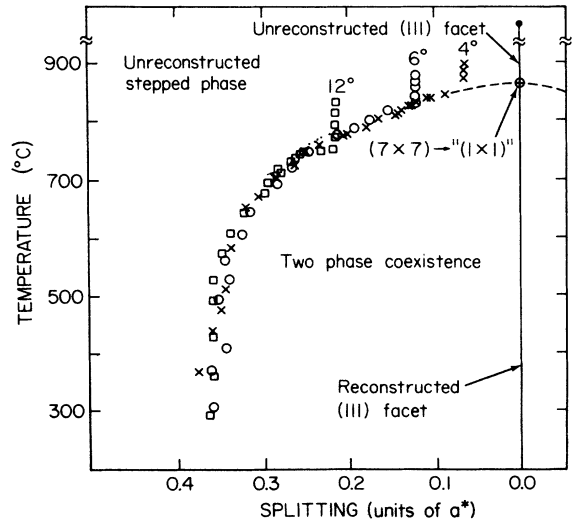

FIG. 7. Measured values of the specular beam splittings, which are proportional to surface misorientation, as a function of temperature for three different net angles of misorientation. Data for the 10° misoriented surfaces (not shown for clarity) fall on the same curve. We have labeled the phases according to our interpretation of the experiment: In particular the dashed line is speculative. The diagram is symmetric about zero splitting. The data shown were measured during cooling. Hysteresis observed for the 12° sample upon warming is shown as solid dots. a^* is defined as in Fig. 3.

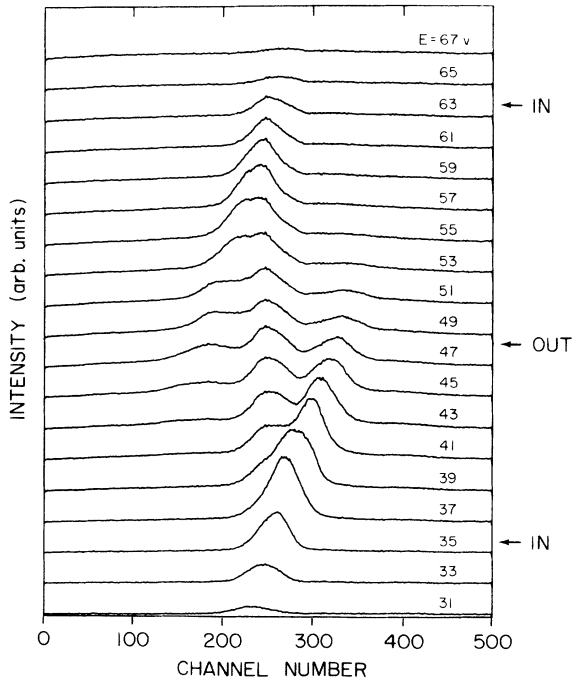

FIG. 8. Angular profiles across the specular beam for a sample misoriented by 6° toward the [2̄11] direction, measured at 817 °C. Angle of incidence is equal to 11°.

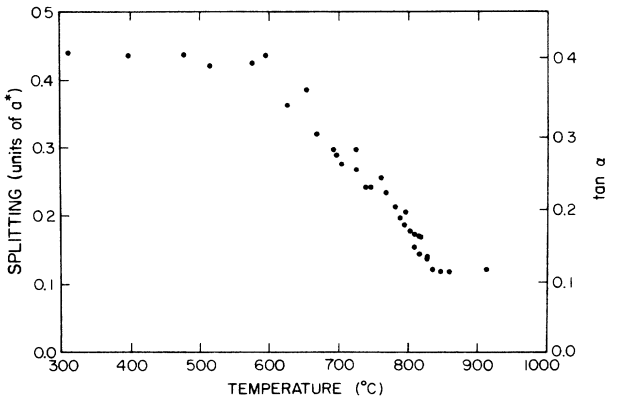

FIG. 9. Separation of the split beams around the specular beam as a function of temperature on the surface misoriented by 6° toward [$\bar{2}$11]. The misorientation α corresponding to the observed splitting is shown on the right-hand axis. As discussed in the text, the uncertainties in the splitting below about 700 °C are large due to incomplete resolution of the split beams and seventh-order beams near out-of-phase conditions.

of-phase conditions indicate this is a rough phase, not a facet.[17]

The temperature dependence of vicinal Si(111) surfaces misoriented toward [$\bar{2}$11] was previously studied by Olshanetsky and Shklyaev.[12] They conclude that below about 800 °C the surface is composed of steps of height twice the interlayer spacing, rather than the coexisting facets and stepped regions we observe. Our data are clearly inconsistent with their conclusion: the periodicity in the perpendicular component of the momentum transfer corresponding to the energy dependence of Fig. 8 would be halved if there were double height steps, i.e., two complete periods of the satellite motion with energy would be observed within this range. A possible source of confusion might have been that at out-of-phase conditions the distances between peaks in the diffracted beam angular profiles just below the phase separation temperature are half of what they are at high temperature because of the presence of the (111) facet beams. This halving is accidental, however: It only occurs at the out-of-phase conditions. Furthermore, as for the misorientations toward the [$\bar{1}$10] and [1$\bar{1}$0], as the temperature is lowered the separation between the split beams increases indicating that they come from a part of the surface whose orientation changes with temperature.

THE TEMPERATURE-ORIENTATION PHASE DIAGRAM AND THE EQUILIBRIUM CRYSTAL SHAPE

A remarkable property of the data in Fig. 7 is that the orientation angle α of the coexisting stepped phase at low temperature is independent of the net orientation. This property substantiates our claim in the previous section that we are observing *phase* coexistence, i.e., the structures observed represent equilibrium configurations. If there were a serious limitation on mass transport, then the orientation of the stepped regions would depend on the net orientation because the amount of mass transport required for the formation of large (111) facets changes with the net misorientation. That we do not see this dependence means that the stepped regions at low temperature are large enough to be thought of as distinct phases. Of course mass transport does play a role at some length scale: the net orientation of the crystal does not change. For the lowest temperatures in Figs. 7 and 9, α stops changing with T. This could be because it actually stops changing in equilibrium, but it seems more likely that at these low temperatures the rate of surface diffusion is becoming sufficiently slow that α is being quenched.[18] As mentioned earlier, a small hysteresis loop in the temperature dependence of α is observed for the 10° and 12° surfaces: The high-temperature phase is evidently metastable on cooling. That only the highest angles studied should show this behavior is not surprising because for these surfaces the transition occurs at the lowest temperatures and thus is more susceptibile to nucleation barriers.

As discussed in the Introduction, another way of representing a phase diagram like Fig. 7 is by plot of the equilibrium crystal shape: The coexistence region at low temperatures represents a sharp edge in the crystal shape. At high temperatures, all (small) α's are evidently allowed, implying that the crystal shape is smoothly curved, with tangent planes at all prepared orientations. Another remarkable feature of Fig. 7 is that the coexistence region, and thus the sharp edge, seems to vanish at roughly the same temperature as the (7×7) to "(1×1)" transition on the flat (111) surface. The coincidence of these two temperatures would suggest a simple thermodynamic mechanism[19] for the appearance of the sharp edge. The following description is in terms appropriate to a first-order process. In this model there are two distinct equilibrium crystal shapes: one on which (local) (7×7) reconstructions appear, and one on which they do not. When compared on a Wulff plot the inner union of these crystal shapes gives the actual stable shape. Our proposed thermal evolution of the two crystal shapes is shown schematically on a Wulff plot in Fig. 10: At high temperatures the equilibrium crystal shape is the one without reconstruction and is smoothly curved away from the (111) facet. Above the (7×7) to "(1×1)" transition, the reconstructed surface always has higher free energy and lies outside of the stable surface on the Wulff plot. If we assume that the reconstructed surface is very stable with respect to the formation of steps, then the reconstructed (111) facet is much larger than the (111) facet on the unreconstructed crystal shape. If no steps are allowed on the reconstructed facet, the behavior will be as in Fig. 10(a). If steps are more weakly unfavorable the model in Fig. 10(b) is appropriate. In either case, on lowering the temperature the crystal shapes first intersect when the facets cross, which is at the temperature of the "(1×1)" to (7×7) transition on the (111) surface. Below the transition temperature the two crystal shapes intersect, forming sharp edges in the equilibrium crystal shape, and resulting in a phase separation as shown in the corresponding phase diagrams. In Fig. 10(b), at lower temperature the point of intersection crosses from the

reconstructed facet to the rounded region. This results in a phase separation between two regions of different step density. In both Figs. 10(a) and 10(b), the phase diagram has the same features near the transition temperature as observed experimentally (see Figs. 7 and 9).

The interpretation of our results in terms of equilibrium thermodynamics would seem questionable if the sizes of the separated phases were very small. Since we see no broadening of the integer-order beams along the direction of misorientation (see, however, the next section), our measurements place a lower limit of perhaps 200–300 Å on the width of the (111) facets at low temperature. Electron microscopy[4] suggests that the (111) facets are microns across and that typically 1000 double-layer steps are clustered together in the misoriented regions which we observe at low temperature. As it is necessary to clean the surfaces by heating to 1250 °C before the faceting is observed, and as the Si sublimation rate at this temperature is large [on the order of 1 Å/sec (Ref. 20)] one might have concluded that these large facets were created during sublimation. However, as we have shown, the facets do not occur until around 800 °C, where the sublimation rate is negligible. The Si surface mobility is evidently large enough to allow facets to form at this temperature.[21]

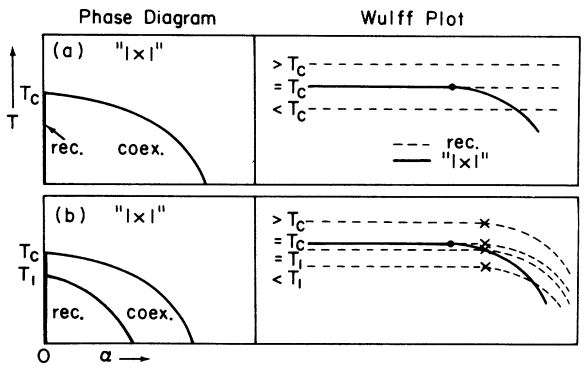

FIG. 10. Wulff plots illustrating the effect of a reconstructive transition on the equilibrium crystal shape, and corresponding temperature-orientation phase diagrams. The solid curves represent the crystal shape with an unreconstructed "(1×1)" facet, and the dashed curves with a reconstructed facet. As temperature decreases, the relative free energy of the reconstructed facet decreases. Below the transition temperature, the two shapes intersect, giving a net equilibrium crystal shape that is the inner envelope of the two. The phase diagram shows regions where all orientations α are allowed for the unreconstructed crystal "(1×1)," regions of phase separation (coex.), and regions where the reconstruction (rec.) is allowed for certain values of α. The relative size of the reconstructed and unreconstructed facets depends on the nature of the interaction between the reconstruction and the steps. Panel (a) shows the behavior for a strongly repulsive interaction. Panel (b) represents a weaker repulsion. Solid circles show the sharp edge at the temperature at which the crystal shapes cross. Crosses show the intersection of the facet and the rounded part of the crystal shape for the reconstructed phase.

THREE-DIMENSIONAL EFFECTS AT LOW TEMPERATURES

Figure 10 is a two-dimensional picture appropriate if the direction of misorientation is perpendicular to an edge in the equilibrium crystal shape. The behavior of the $[\bar{2}11]$ misoriented sample appears consistent with this description, as does that of the $\pm[\bar{1}10]$ misoriented samples above approximately 700 °C. However, below 700 °C the $\pm[\bar{1}10]$ samples undergo additional changes in structure indicative of the three-dimensional nature of the equilibrium crystal shape. Figure 11 is a picture of the LEED pattern for the 12° orientation at 350 °C. Three new features have appeared. First, the split beams have rotated from the $[\bar{1}10]$ direction approximately 8° in the $+\delta$ direction of Fig. 1. The direction of this rotation is the same for all the samples, indicating it is not an artifact of the initial small deviations from the $[1\bar{1}0]$ direction. (This discussion and Fig. 11 are appropriate for the 4°, 10°, and 12° samples. The pattern for the 6° sample, which is misoriented toward the $[1\bar{1}0]$, can be obtained by reflecting through the $(1\bar{1}0)$ plane.) The temperature dependence of the rotation is shown in Fig. 12. The second new feature in the LEED pattern is the appearance of two new satellite beams [most easily seen in Fig. 11 for the $(1\bar{1})$ and (01) beams] around the integer-order beams. The inset in Fig. 13 shows the satellite beams, along with the directions needed for our discussion of them; the solid dots represent seventh-order beams, the hollow dots the satellite beams. The new, "secondary" satellite beams are displaced from the original, "primary" satellite beams by $\pm\mathbf{B}^*$ (Fig. 13) and are approximately half as intense. These new features evolve over the same temperature range as the rotation (see Fig. 12). They appear first as a broadening and then as "spurs" of intensity at the edges of the original satellite beams. These spurs develop into resolved satellites which migrate monotonically, roughly along the $\mathbf{B}^*$ direction, with decreasing temperature to their final positions. This migration ceases at the same temperature as that at which the rotation of the primary satellite azimuth saturates. Finally,

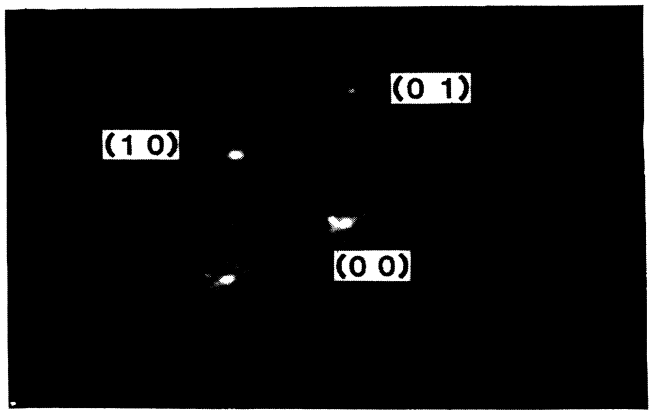

FIG. 11. LEED pattern from Si(111) misoriented by 12° toward the [110] at room temperature. Incident energy is equal to 42 eV, incident angle is equal to 9°.

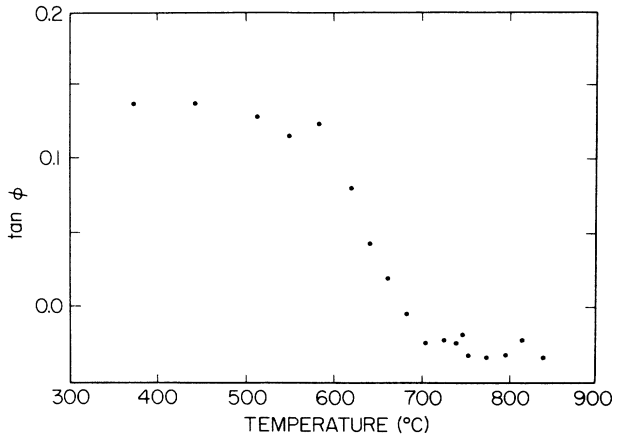

FIG. 12. Temperature dependence of the rotation of the split beam azimuth on the sample misoriented by 12° toward the $[\bar{1}10]$ direction. Measured for the $(1\bar{1})$ beam at angle of incidence is equal to 8°; incident energy is equal to 44 eV (out-of-phase condition). The curve is reversible.

the third new feature in the LEED pattern of Fig. 11 is diffuse streaks of intensity along those azimuths which connect near-neighbor integer-order beams and run parallel to the $[\bar{1}2\bar{1}]$ direction. In the vicinity of the integer-order beams the streaks are not evident at calculated monoatomic-height step in-phase conditions, and are most pronounced at calculated out-of-phase conditions. In addition, for the 12° net misoriented surface, a slight broadening of the integer-order beams along the $[\bar{1}2\bar{1}]$ direction is observed.

Significantly, as seen in Figs. 11 and 13, $\mathbf{A}^*$ no longer points in the $[\bar{1}10]$ direction: It is rotated by an angle ϕ. By varying the incident electron energy, we observe that the positions of both the primary and secondary satellites relative to the integer-order positions move along the $\mathbf{A}^*$ direction, as shown in Fig. 14. The vectors $\mathbf{A}^*$ and $\mathbf{B}^*$, derived from mapping the observed satellite positions into reciprocal space coordinates, are constant to within the uncertainties of the determination. The lattice vectors $\mathbf{A}=4\mathbf{a}/3-7\mathbf{b}/3-\mathbf{c}$ and $\mathbf{B}=3\mathbf{a}+8\mathbf{b}$, shown in Fig. 13, produce the best overall fit to the observed reciprocal lattice vectors $\mathbf{A}^*$ and $\mathbf{B}^*$ for the 12° sample below about 500 °C, where they stop changing. The satellite motion with energy yields a period in the perpendicular component of the momentum transfer very close to that observed at high temperature.

The rotation of the vector $\mathbf{A}^*$, which occurs without a change in its energy dependence, indicates that the original step edges have rotated by the angle ϕ without a change in height. The correlated motion of the secondary satellites shows that the reciprocal-lattice rods of the primary and secondary satellites are parallel and are almost certainly associated with the same step structure; this indicates a periodic structure with lattice vector $\mathbf{B}$ parallel to the step edges. Using these assumptions, the magnitudes and directions of $\mathbf{A}^*$ and $\mathbf{B}^*$ have been calculated, and are compared with the measured values in Table I. The calculated energy dependence of the satellite beams over an entire in-phase, out-of-phase, in-phase period is shown as the solid lines in Fig. 14.

The periodicity parallel to the step edge can arise from a reconstruction on the terraces or from an ordered array of kinks along the step edge. In view of the low symmetry of the step edge, the latter seems likely. In Fig. 13, we show one possible model for such a kink structure. The model consists of alternating $[\bar{2}11]$ and $[\bar{1}2\bar{1}]$ edges with a repeat vector $\mathbf{B}$. A very crude kinematical intensity calculation which includes scattering from only the topmost double layer of atoms suggests that this kink arrangement more closely reproduces the observed primary-to-secondary intensity ratio than an arrangement made up of either alternating $[\bar{2}11]$ and $[\bar{1}10]$ edges or $[\bar{2}11]$ and $[11\bar{2}]$ edges. The calculation gives a ratio of

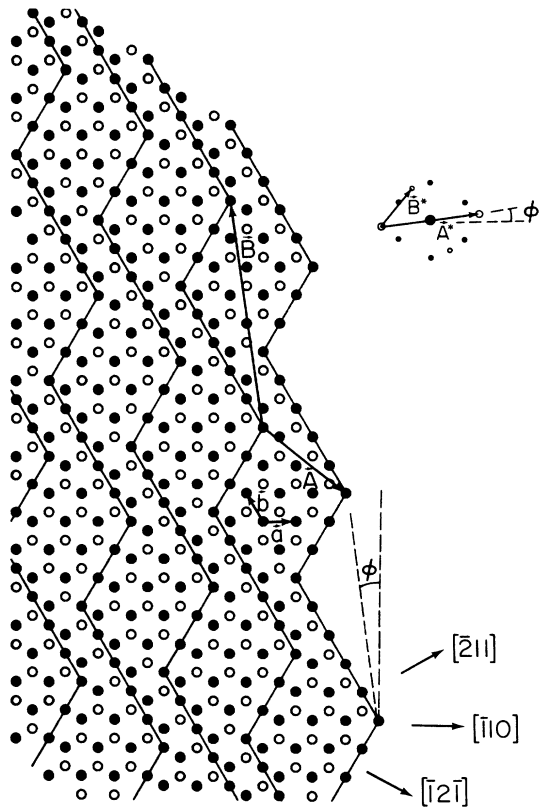

FIG. 13. Inset: Schematic drawing of the beams near an integer-order position from the pattern of Fig. 11. The large solid spot is the integer-order beam, the small solid spots are seventh-order beams. The large open circles are the original satellite (split) beams which have rotated by an angle ϕ with respect to the $[\bar{1}10]$ direction. They are separated by the reciprocal-lattice vector $\mathbf{A}^*$. The small open circles are the new satellites, and are positioned with respect to the original satellite beams with reciprocal lattice vector $\mathbf{B}^*$. In the main figure, the real space coordinates $\mathbf{A}$ and $\mathbf{B}$ correspond to the diffraction pattern. Open circles represent the top layer of Si atoms, closed circles the second layer and straight lines the step edges. The step edge orientation has rotated by an angle ϕ and a periodicity corresponding to the reciprocal-lattice vector $\mathbf{B}^*$ exists parallel to the step edge. A plausible origin for this periodicity is a kink structure along the step edges as shown.

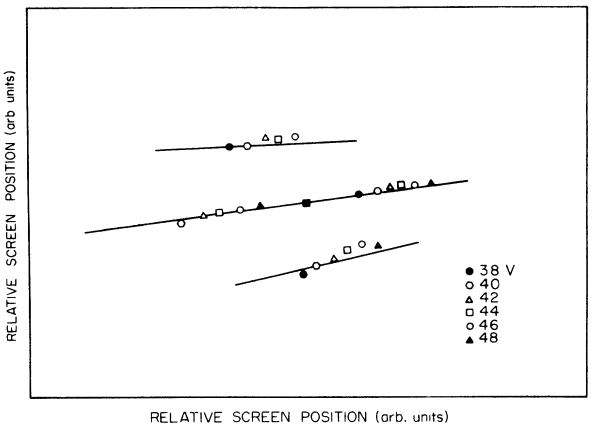

FIG. 14. Motion of the satellite beams with respect to the integer-order beam (solid square) as observed as a function of energy. Incident energies as indicated in the figure. Measurement is for the $(1\bar{1})$ beam. Incident angle is equal to 8° towards $[1\bar{1}0]$. The solid line shows the calculated energy dependence over an entire in-phase, out-of-phase, in-phase period for the lattice vectors of Fig. 13, corresponding to an energy range of 32 to 56 V. Overall scale is determined via measurement of the screen positions of neighboring seventh-order reflections, relative to the integer-order position.

~4:1 for the illustrated model compared to an observed 2:1 ratio. However, this is certainly not a unique determination of the structure. Furthermore, the ordered arrangement of Fig. 13 represents only an average structure. The satellites are broader than the instrument limited angular width, indicating some spread in the distribution of lattice vectors **A** and **B**.

The rotation of the steps away from the $[\bar{1}10]$ direction below 700 °C implies that other parts of the surface must have compensating misorientation so as to keep the total misorientation fixed. We hypothesize that the streaks observable in Fig. 9 are due to these compensating regions.

TABLE I. Calculated vs. measured reciprocal lattice vectors. The first column contains calculated magnitudes $\mathbf{A}^*$ and $\mathbf{B}^*$, the rotation azimuth, ϕ, the angle between $\mathbf{A}^*$ and $\mathbf{B}^*$, γ, and the angle between the surface normal and [111], α, for the lattice vectors of Fig. 13. The second column, to be compared with the measured values, contains values corrected for the inclination angle α. The third column contains "measured" values in the (111) plane, derived by mapping observed satellite positions into reciprocal space coordinates.

	Calculated from model	Calculated value in (111) plane	Measured
$\lvert\mathbf{A}^*\rvert/\lvert\mathbf{a}^*\rvert$	0.371	0.396	0.37±0.03
$\lvert\mathbf{B}^*\rvert/\lvert\mathbf{a}^*\rvert$	0.176	0.182	0.185±0.02
ϕ	8.2°	8.2°	8°±1°
γ	44.7°	42.8°	43°±3°
α	20.4°		

Such streaks can arise from regions misoriented towards the $[\bar{1}2\bar{1}]$ direction which are composed of very disordered step arrays.[22] This interpretation is supported by our observations of an energy dependence for the streaks consistent with monoatomic-height steps.

There are at least two possibilities for how this $[\bar{1}2\bar{1}]$ misoriented phase could enter the phase diagram. First it could represent a third coexisting phase; the surface misoriented towards the $[\bar{1}2\bar{1}]$ could coexist with the (111) facet and the kinked surface. The possible existence of a region of three-phase coexistence at low temperature is not surprising. Three-phase coexistence corresponds to a sharp corner on the equilibrium crystal shape. At zero temperature, when the crystal shape is completely faceted, surfaces oriented in nonhigh symmetry directions (such as the $\pm[\bar{1}10]$) will only be "tangent" to the equilibrium crystal shape at a sharp corner. The other possibility is that there are still only two coexisting phases; i.e., the (111) facet has been replaced by the $[\bar{1}2\bar{1}]$ misoriented stepped surface in a second transition as illustrated in Fig. 10(b). In this picture a sharp edge separates two types of stepped surface rather than a facet and a stepped surface. Under either of these interpretations, that we resolve no splitting of the specular beam in the $[\bar{1}2\bar{1}]$ direction at any energy indicates that the steps are too far apart for our instrument to detect, or that there is considerable disorder in the step-step correlations. A slight broadening of the specular beam observed along the $[\bar{1}2\bar{1}]$ direction of the 12° misoriented samples is consistent with a low step density just at the limits of observability with our resolution. The thermal evolution of the diffraction pattern is also consistent with either of these interpretations. The diffuse streaks and the extra beams only appear when the azimuth containing the original beams begins to rotate from the $[\bar{1}10]$ direction. Higher resolution measurements of the beam profiles to determine the magnitude of the misorientation toward the $[\bar{1}2\bar{1}]$, as well as measurements of the thermal evolution of surfaces misoriented toward the $[\bar{1}2\bar{1}]$, direction are needed for a more complete understanding of this three-dimensional behavior. This work is in progress.

CONCLUSION

We have studied the structure of vicinal Si(111) surfaces using kinematical low-energy electron diffraction. The increasing complexity of the LEED patterns observed at lower temperature emphasizes the necessity to examine the shape of the diffracted intensity reflections as a function of energy (and thus the perpendicular component of the momentum transfer), in addition to angular position, in order to fully characterize a structural phase transition. Qualitative differences in our results for misorientations toward $[\bar{1}10]$, $[\bar{2}11]$, and $[2\,\bar{1}\,\bar{1}]$,[22] make clear the further need to examine a variety of orientations to understand the three-dimensional surface structure of nonhigh symmetry orientations.

At temperatures above the (7×7) to "(1×1)" transition, the LEED pattern indicates that vicinal Si(111) surfaces consist of a single stepped phase. The energy dependence of the integer-order reflection angular

profiles is consistent with predominantly monoatomic height steps and wandering step edges, as expected from entropic considerations. On surfaces misoriented toward the $\pm[1\bar{1}0]$ or the $[\bar{2}11]$ directions, the onset temperature of the (7×7) reconstruction decreases monotonically with net misorientation. This transition coincides with a reversible phase separation of the surface into reconstructed unstepped regions and unreconstructed stepped regions,[23] which must occur via migration of Si atoms across the surface. The phase separation is driven by the formation of a sharp edge in the Si equilibrium crystal shape, and can be understood via a picture of intersecting reconstructed and unreconstructed crystal shapes, as shown in Fig. 10. In this model, the specific form of the observed phase diagram arises due to an unfavorable interaction between the reconstruction and the step edge. Many different types of phase diagrams can be predicted for different step-reconstruction interactions. Such observations may serve as a severe test for models describing the energetics of semiconductor surfaces.[24]

The surfaces misoriented toward the $\pm[\bar{1}10]$ and toward the $[\bar{2}11]$ behave similarly down to 700 °C. However, at approximately 700 °C, a second transition occurs on the $\pm[\bar{1}10]$-misoriented surfaces, resulting in the coexistence of two types of steps on the surface. Thus the tangent planes for these misorientations either cut across a sharp corner or a sharp edge between rounded parts in the equilibrium crystal shape. Observations of a single stepped phase at low temperature for a surface misoriented toward $[\bar{1}\,\bar{1}\,2]$ favor the latter model.[22]

ACKNOWLEDGMENTS

We thank the Laboratory for Physical Sciences for providing the facilities with which the experiments were performed. This work was supported by the U.S. Department of Defense (DOD) and by the National Science Foundation (NSF) under Grant No. DMR-85-04163.

[1]C. Rottman and M. Wortis, Phys. Rep. **103**, 59 (1984); M. Wortis, in *Chemistry and Physics of Solid Surfaces,* edited by R. Vanselow and R. Howe (Springer-Verlag, Berlin, 1988), Vol. VII.

[2]C. Herring, Phys. Rev. **82**, 87 (1951).

[3]Careful recent studies have been mostly confined to small (1–10 μm) metal crystals (Pb, Au, In) and to 1–5-mm hcp ^{4}He crystals in coexistence with the superfluid near 1 K. See Ref. 1 for relevant references.

[4]Y. Ishikawa, N. Ikeda, M. Kenmochi, and T. Ichinokawa, Surf. Sci. **159**, 256 (1985).

[5]R. S. Becker, J. A. Golovchenko, E. G. McRae, and B. S. Swartzentruber, Phys. Rev. Lett. **55**, 2028 (1985).

[6]N. Osakabe, Y. Tanishiro, K. Yagi, and G. Honjo, Surf. Sci. **109**, 353 (1981).

[7]W. Telieps, Appl. Phys. **A44**, 55 (1987); E. Bauer and W. Telieps, Scanning Electron Microsc. Suppl. **1**, 99 (1987).

[8]K. Takayanagi, Y. Tanishiro, M. Takahashi, and S. Takahashi, J. Vac. Sci. Technol. **A3**, 1503 (1985).

[9]J. C. Phillips, Phys. Rev. Lett. **45**, 905 (1980); see also, however, D. Vanderbilt, Phys. Rev. Lett. **59**, 1456 (1987).

[10]H. J. Gossman, J. C. Bean, L. C. Feldman, E. G. McRae, and I. K. Robinson, Phys. Rev. Lett. **55**, 1106 (1985).

[11]M. C. Payne, J. Phys. C **20**, L983 (1987).

[12]B. Z. Olshanetsky and A. A. Shklyaev, Surf. Sci. **82**, 445 (1979).

[13]R. J. Phaneuf and E. D. Williams, Phys. Rev. Lett. **58**, 2563 (1987).

[14]R. J. Phaneuf and E. D. Williams, in *The Structure of Surfaces II,* edited by J. F. van der Veen and M. A. Van Hove (Springer-Verlag, Berlin, in press).

[15]W. P. Ellis and R. L. Schwoebel, Surf. Sci. **11**, 82 (1968).

[16]M. Henzler, Surf. Sci. **22**, 12 (1970); M. Henzler, in *Electron Spectroscopy for Surface Analysis,* edited by H. Ibach (Springer-Verlag, Berlin, 1977), p. 117.

[17]B. Z. Olshanetsky and V. I. Mashanov, Surf. Sci. **111**, 414 (1981).

[18]In previous work [R. J. Phaneuf and E. D. Williams, Surf. Sci. **195**, 330 (1988)], we have laser-quenched the high-temperature phase to room temperature. We find that the step structure begins to change after heating to 400 °C; after heating to 750 °C it reverts back to its equilibrium structure. See Y. J. Chabal, J. E. Rowe, and S. B. Christman, Phys. Rev. B **24**, 3303 (1981) for similar observations on $[11\bar{2}]$ misoriented surfaces.

[19]J. W. Cahn, J. Phys. (Paris) Colloq. **12**, C6-199 (1982).

[20]J. L. Souchière and V. T. Binh, Surf. Sci. **168**, 52 (1986).

[21]Observations of surface morphology changes, such as faceting, are important sources of information about surface self-diffusivities [see, for example, H. P. Bonzel, in *Surface Mobilities on Solid Materials,* edited by Vu Thien Binh (Plenum, New York, 1983), p. 195]. It is difficult, however, for us to intepret our data quantitatively in terms of diffusivities because of the lack of information about the size of the facets in our experiment.

[22]Indeed, the streak seems to be characteristic of surfaces misoriented toward the $\langle\bar{1}2\bar{1}\rangle$ direction: R. J. Phaneuf and E. D. Williams (unpublished).

[23]In the electron microscopy studies of Refs. 6 and 7, steps were observed which were separated by thousands of Å. These steps do not show the tendency to cluster and form a separate stepped phase at low temperatures as we observe for much higher step densities. Two conclusions are possible as to the source of this difference. The first is that surfaces with low step densities are stable with respect to faceting. The other is that the kinetics of step clustering is slow for small step densities. The latter possibility seems likely because of the large, and seemingly very unlikely, fluctuations needed for a step to recognize the presence of other steps.

[24]F. H. Stillinger and T. A. Weber, Phys. Rev. B **31**, 5262 (1985); J. Tersoff, Phys. Rev. Lett. **56**, 632 (1986); B. W. Dodson, Phys. Rev. B **36**, 1068 (1987); R. Biswas and D. R. Hamann, Phys. Rev. Lett. **55**, 2001 (1985).

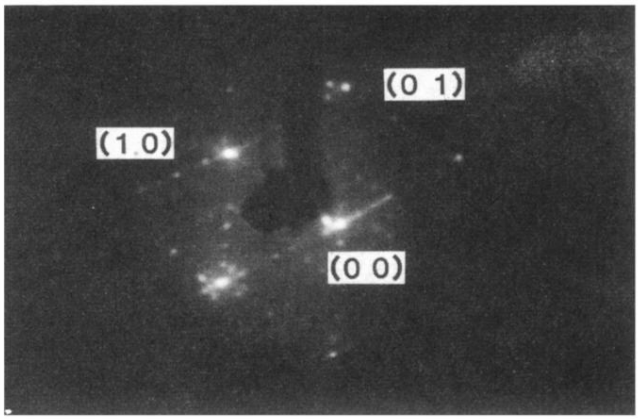

FIG. 11. LEED pattern from Si(111) misoriented by 12° toward the [110] at room temperature. Incident energy is equal to 42 eV, incident angle is equal to 9°.

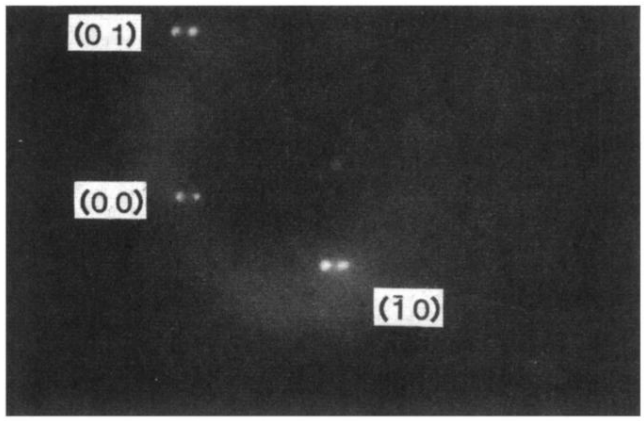

FIG. 2. LEED pattern from Si(111) misoriented by 6° toward [1$\bar{1}$0] at 845 °C. Incident energy is equal to 47 eV; incident angle is equal to 7° from the [111] direction.